Tribol Lett
DOI 10.1007/s11249-012-0100-z

ORIGINAL PAPER

Friction-Induced Vibration by Stribeck's Law: Application to Wiper Blade Squeal Noise

J. Le Rouzic · A. Le Bot · J. Perret-Liaudet · M. Guibert · A. Rusanov · L. Douminge · F. Bretagnol · D. Mazuyer

Received: 3 October 2012 / Accepted: 27 December 2012

Abstract This paper is concerned with the squeal noise of a wiper/windscreen contact. It is shown that squeal noise stems from friction-induced self-excited vibrations in the context of Stribeck's law for friction coefficient. The study is specifically focussed on the instability range of velocities and not on the amplitude of limit cycles. The studied dynamic system consists of a single degree-of-freedom mass-spring-damper oscillator submitted to a velocity-dependent frictional force which follows the Stribeck law. The local stability is analyzed by the first Lyapunov method and results in a stability criterion. Experiments have been performed on a glass/elastomer contact lubricated with water. The tribometer 'LUG' provides measurements of the vibrational velocity and friction force versus sliding speed. It is found that the instability appears during the transition between boundary and elastohydrodynamic regimes where the negative gradient of the friction versus velocity curve is steep. The apparition and vanishing of instability are correctly predicted by the steady-state stability criterion.

Keywords Elastomers · Glass · EHL (General) · Stick-slip

1 Introduction

Car windscreen wiper blades are widely used in the automotive industry. The main function of such a system is to remove water (or bugs) from a car windscreen by a reciprocating motion. A rubber blade with a specific shape acts as a moving seal on the glass with a surface contact area of only few tens of microns. The mechanisms governing the tribological interaction between rubber wiper blades and vehicle windscreens are relatively complex [1] in comparison to their primary function (removing water from glass). Optimizing the performance of wiper blades [2] and decreasing their friction [3, 4] are still important challenges. Moreover, as automobiles become more and more soundless, with electrical motors for example, an emerging request from customers is to produce rubber wiper blades with reduced noise emission.

Among the large variety of frictional noises that may be encountered in nature and industrial mechanisms [5], the squeal noise and its initiation have received special attention from researchers [6]. For example, in [7] the squeal noise of a waist seal of the lateral door of a car is studied by a finite element approach. Indeed, self-excited vibrations in frictional oscillators have been widely studied in the literature, as typical examples of nonlinear oscillators [8, 9]. The usual system is modelled as a mass attached to a frame by a spring and a damper which slides on a conveyor belt. This classical approach leads one to notice that the presence of a transition in friction can make the steady-state unstable. The most studied example is the stick-slip phenomenon [10–13] which occurs in systems where the static friction coefficient is greater than the kinematic friction coefficient.

Even though the nature of the stick-slip oscillations and the transition from stable sliding to unstable sliding are very different according to the nature of the contact, they have common characteristics. Their dynamics is determined by intrinsic properties of the surface layers. Most of the experiments reported in the literature are carried out

J. Le Rouzic (✉) · A. Le Bot · J. Perret-Liaudet · M. Guibert · A. Rusanov · L. Douminge · D. Mazuyer
LTDS-UMR 5513 CNRS-Ecole Centrale de Lyon, 36 Avenue Guy de Collongue, 69134 Ecully Cedex, France
e-mail: j.le-rouzic@imperial.ac.uk

F. Bretagnol
Valeo Systèmes d'essuyage, 63500 Issoire, France

Published online: 18 January 2013

within over-damped conditions in which the response time of the mechanical system is much shorter than characteristic slip time of the interface itself. Their friction trace is governed by long memory distances. This first indicates the presence of slip domains or long-range cooperativity extended over lateral distances huge compared with molecular dimensions. As the associated relaxation times are much retarded by the effect of pressure, a detailed description of the sliding history is required to obtain a complete picture of the physical shear processes and to be able to predict how the system will accommodate a change of tribological conditions. These memory effects that link the microscopic and the macroscopic scales in friction processes are the basis of the so-called phenomenological rate and state models to describe the frictional response of dry/boundary lubricated single or multi-asperity contacts as initiated by Ruina for friction of rocks [14]. The rate variable refers to the instantaneous sliding velocity and the state variable is meant to capture all the history dependent effects. This approach assumes that the interfacial area is large enough to be self-averaging. Therefore, the mean-field state variable is sufficient to model collective dependence of friction both on the internal degrees of freedom of the interfacial materials and on the dynamical variables characteristic from the shear motion. That is why by relating the state variable to the average lifetime of individual contacts, Ruinas constitutive equations have been successfully applied to dry friction between solids with micron scale roughness [15–18] but are not relevant in wet or lubricated contact.

Although the transition from static to kinetic friction always raises some questions [19], the mathematical description of the instability is well understood. Rubber wiper blades are known to produce different noises that can be classified in three main groups, squeal, chattering and reversal noise. In Ref. [20], the noise is linked to the reversal behaviour of the blade. In Ref. [21], the origin of the squeal noise of a wiper blade is attributed to the velocity weakening of friction coefficient induced by a geometrical effect. But in Ref. [22] the role of lubricated regime on the occurence of the instability is underlined. This is also highlighted in other tribological systems [23].

In this paper, the squeal noise of windscreen wiper blades is studied with an emphasis on the tribological origin of the instability. Specific attention is paid to squeal noise apparition and vanishing in wet conditions as a function of steady-state Stribeck's law. Indeed, over the past decades, many authors have shown that steady-state velocity-friction laws are not valid in dynamic measurements as soon as self-excited vibrations appear [24–27]. Nevertheless, the paradoxal approach used here is to derive the steady-state Stribeck's law when the system is still stable (and Stribeck's law valid) to predict the Hopf bifurcation. It has been shown in Ref. [22] that for a given sliding velocity, the lifetime, the size and the number of the contacting spots does not depend on the stability of the friction regime. This experimental result supports the use of our approach. Our objective is then to predict the range of unstable velocities even if the limit cycles cannot be estimated.

The paper is organized as follows. In Sect. 2 the stability of a damped-spring-mass oscillator subjected to a frictional force following Stribeck's law is studied. In particular, the stability criterion is derived. In Sect. 3 an experiment on a wiper blade / glass disc is described. The contact is lubricated with water. Experimental results were performed to verify the theoretical prediction of the stability range. Stribeck curves are obtained while instabilities are observed thanks to vibration measurements. The theoretical prediction of the stability range is compared with experimental observation of the squeal noise.

2 Modelling

2.1 Dynamical System

Let us consider a solid of mass m at position x attached to a rigid foundation by a spring of stiffness k and viscous damping ratio c. The solid is sliding on a conveyor belt with speed V as shown in Fig. 1.

At the conveyor-mass interface, a friction force $T(v)$ which depends on the relative velocity $v = V - \dot{x}$ is applied. The governing equation for the transverse motion of the oscillator is

$$m\ddot{x} + c\dot{x} + kx = T(V - \dot{x}) \quad \text{for } \dot{x} \neq V \tag{1}$$

$$\dot{x} = V \quad \text{for } |kx| \leq T(0) \tag{2}$$

The first equation applies whenever the relative velocity is non-zero $\dot{x} \neq V$ (slip condition) whereas the second equation applies if the elastic force kx is lower than the static friction force $T(0)$ (stick condition). However, in the case of a wiper-windscreen contact, the instability is observed about a non-zero sliding velocity and the

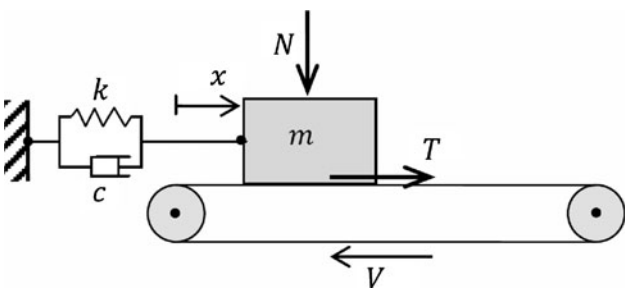

Fig. 1 Friction-induced vibration of a mass spring oscillator

vibrational velocity $\dot{x}$ never reaches the sliding velocity V so that $|\dot{x}| < V$. This condition will be checked in the experiment (as stick-slip type friction-induced vibration never occurs in our experiments). The equality $\dot{x} = V$ is, therefore, never fullfilled and we confine the study to the first equation. The friction force may be written as the product $\mu_k\ N$ where N is the normal load and $\mu_k(v)$ the kinetic friction coefficient,

$$T(v) = \mu_k(v) N \mathrm{sgn}(v) \tag{3}$$

where sgn(v) denotes the sign of the relative velocity v. Since we have assumed $v = V - \dot{x} > 0$, the sign function may be removed from the above.

2.2 Dimensionless Equation

By setting the natural frequency $\omega^2 = k/m$ and the damping ratio $\zeta = c/2m\omega$, one can introduce the dimensionless time $\tau = \omega\ t$ and displacement $q = kx/N$. Equations (1) and (3) then become,

$$q'' + 2\zeta q' + q = \mu(\tilde{v}) \quad \text{whenever } |q'| < \tilde{V} \tag{4}$$

where prime denotes the derivative with respect to the dimensionless time τ. The dimensionless velocities are given by $\tilde{v} = kv/\omega N$ and $\tilde{V} = kV/\omega N$. They are related by,

$$\tilde{v} = \tilde{V} - q' \tag{5}$$

$\mu(\tilde{v}) = \mu_k(\omega N \tilde{v}/k)$ is the friction coefficient function of the dimensionless velocity.

2.3 Stability Analysis

For a given dimensionless sliding velocity $\tilde{V}$, the equilibrium state is,

$$q_0'' = 0;\ q_0' = 0;\ q_0 = \mu(\tilde{V}) \tag{6}$$

This equilibrium state (stable node or focus) is associated to a stationary slip where the conveyor belt moves at speed $\tilde{V}$ but not the oscillator ($q_0{}' = 0$). The equilibrium may be stable or unstable. As it is well known for this kind of friction-induced self-excited oscillator that the equilibrium state can undergo instability through a Hopf bifurcation leading to a cycle solution, i.e. a periodic vibration. This stability problem may be analyzed by the first Lyapunov method.

To this end, the problem is reconsidered in the phase space by introducing the momentum p,

$$p = q' \tag{7}$$

Equation (4) then reduces to the first order differential equation,

$$\begin{pmatrix} q' \\ p' \end{pmatrix} = \begin{pmatrix} 0 & 1 \\ -1 & -2\zeta \end{pmatrix} \begin{pmatrix} q \\ p \end{pmatrix} + \begin{pmatrix} 0 \\ \mu(\tilde{V} - p) \end{pmatrix} \tag{8}$$

The Jacobian matrix evaluated at (q_0, $p_0 = 0$) is

$$[J] = \begin{pmatrix} 0 & 1 \\ -1 & -2\zeta - \frac{d\mu}{d\tilde{v}}(\tilde{V}) \end{pmatrix} \tag{9}$$

Stability is ensured when all eigenvalues of $[J]$ lie in the complex half-plane $\Re(z) < 0$ and the system is unstable if at least one eigenvalue belongs to the half-plane $\Re(z) > 0$. But the eigenvalues $\lambda_i,\ i = 1, 2$ of $[J]$ are

$$\lambda_i = -\left(\zeta + \frac{1}{2}\frac{d\mu}{d\tilde{v}}\right) \pm \imath\sqrt{1 - \left(\zeta + \frac{1}{2}\frac{d\mu}{d\tilde{v}}\right)^2} \quad \text{if } \left|\zeta + \frac{1}{2}\frac{d\mu}{d\tilde{v}}\right| \leq 1 \tag{10}$$

$$\lambda_i = -\left(\zeta + \frac{1}{2}\frac{d\mu}{d\tilde{v}}\right) \pm \sqrt{\left(\zeta + \frac{1}{2}\frac{d\mu}{d\tilde{v}}\right)^2 - 1} \quad \text{otherwise} \tag{11}$$

where the derivative $d\mu/d\tilde{v}$ is taken at $\tilde{V}$. The positions of the eigenvalues in the complex plane are plotted in Fig. 2. It is clear from these expressions that if $2\zeta + d\mu/d\tilde{v} < 0$ then $\Re(\lambda_i) > 0$ for $i = 1{,}2$ (unstable) but if $2\zeta + d\mu/d\tilde{v} > 0$ then $\Re(\lambda_i) < 0$ for $i = 1{,}2$ (stable). Furthermore, the passage from the left half-plane $\Re(z) < 0$ to the right half-plane $\Re(z) > 0$ occurs through the imaginary axis $\Im(z) = 0$ simultaneously by the two complex conjugate eigenvalues, this is a Hopf bifurcation.

In conclusion, if

$$\frac{d\mu}{d\tilde{v}}(\tilde{V}) < -2\zeta \tag{12}$$

the equilibrium is unstable and leads to a periodical response, i.e. a limit cycle. The equilibrium is stable if $d\mu/d\tilde{v}(\tilde{V}) > -2\zeta$.

2.4 The Case of Stribeck's Law

The previous stability analysis is valid for any model of the friction force $T(v)$ but in this study we consider the case of Stribeck's law. As it is hard to estimate the derivative of friction from measured raw data, using an analytical

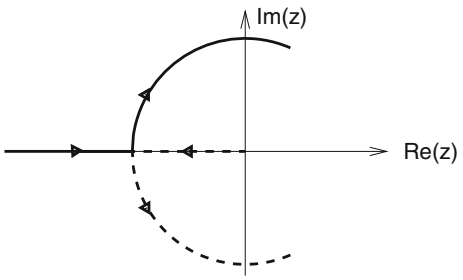

Fig. 2 Qualitative evolution of eigenvalues of Eqs. (10, 11) in complex plane for increasing values of $\zeta + 1/2 \times d\mu/d\tilde{v}$

expression to fit the curve is more accurate. Several models can be found in the literature, including cubic polynomial or exponential models [28] but the more efficient results in our case have been obtained with Bongaerts *et al.*[29] fit.

Following Bongaerts *et al.*, the Stribeck law is expressed as follows,

$$\mu_k(v) = \mu_E(v) + g_T(v)(\mu_B(v) - \mu_E(v)) \tag{13}$$

where $\mu_E(v)$ represents the elasto-hydrodynamic lubrication (EHL) regime, $\mu_B(v)$ is the boundary regime while the function $g_T(v)$ connects these two regimes (i.e. the transitional mixed regime). At low velocities, the friction coefficient is high and varies very little with velocity (boundary regime). Contacts between asperities are possible and solid/solid interactions are predominant in the friction. The mixed regime characterises the velocity range during which the friction coefficient quickly decreases with increasing speed. At high velocities the EHL regime finally arises with a low friction coefficient, where a liquid film is formed between the surfaces.

As can be observed experimentally, the friction coefficient for both EHL and boundary regimes may be described by a simple power law,

$$\mu_B(v) = G \cdot (v\eta)^l \tag{14}$$

and

$$\mu_E(v) = H \cdot (v\eta)^n \tag{15}$$

In these relationships, η is the lubricant viscosity, G and l are, respectively, the boundary power-law coefficient and exponent, and H and n similar coefficients for the EHL regime. Finally, the transition function $g_T(v)$ may be introduced as,

$$g_T(v) = \frac{1}{1 + (v\eta/U)^r} \tag{16}$$

where U is the value of $v\eta$ under which the boundary regime dominates and r is the exponent characterising the mixed regime. The Stribeck law then reads

$$\mu_k(v) = H(v\eta)^n + \frac{1}{1 + (v\eta/U)^r}\left(G(v\eta)^l - H(v\eta)^n\right) \tag{17}$$

In a dimensionless form, the friction coefficient becomes

$$\mu(\tilde{v}) = \left[\tilde{H}\tilde{v}^n + \left(\frac{1}{1 + (\tilde{v}/\tilde{U})^r}\right)\left(\tilde{G}\tilde{v}^l - \tilde{H}\tilde{v}^n\right)\right] \tag{18}$$

An example of this type of curve is shown in Fig. 3. The three regimes are clearly apparent in this figure. The boundary regime is a flat curve of constant level ($l = 0$). The constant G can be read from this figure as the value of μ for a zero sliding speed.

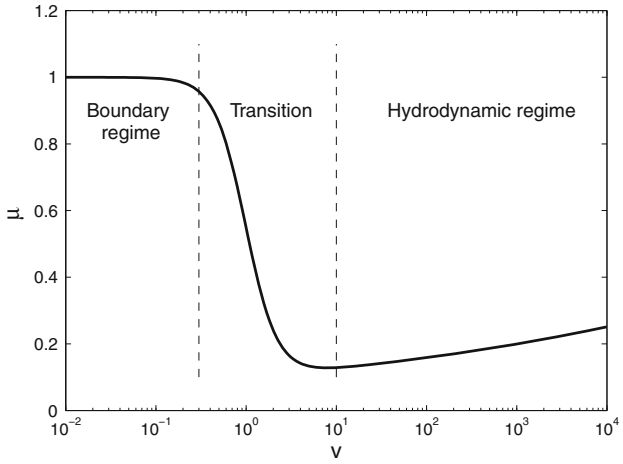

Fig. 3 Stribeck master curve in dimensionless form $\mu(\tilde{v})$ for $G = 1$; $l = 0$; $H = 0.1$; $n = 0.1$; $U = 1$; $r = 2.5$

The first derivative of μ with respect to $\tilde{v}$, which can be easily obtained from the fit curve, is shown in Fig. 4. The unstable regime is reached when the slope $d\mu/dv(\tilde{v})$ is lower than a fixed level, worked out by the appartion of instability (for example, $\zeta = 0.1$ in Fig. 4).

Knowing the viscous damping coefficient ζ, it is then easy to predict the velocity range of $\tilde{v}$ for which the equilibrium state is unstable, leading to a periodical limit cycle response.

3 Experiment

In order to check the relevance of the above theoretical results, sliding friction tests of elastomer wiper blades samples against glass disc lubricated with water have been performed. Vibration velocity and displacement have been recorded during friction tests.

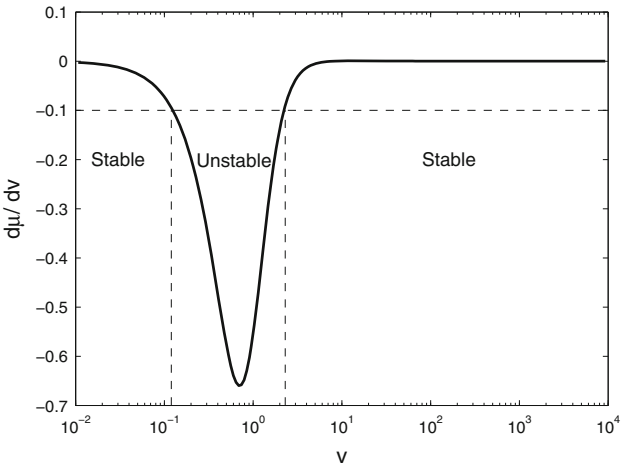

Fig. 4 First derivative $d\mu/dv(\tilde{v})$ of the Stribeck master curve shown in Fig. 3

3.1 Experimental Setup

To study dynamic phenomena occuring in lubricated contacts, LTDS has developed a specific apparatus called 'LUG' (Fig. 5). It is composed of a fixed aluminium plate attached to a concrete bloc supported by 4 air springs. The high mass (600 kg) obtained with this construction allows low resonant frequencies of the whole bench. At the center of the top plate, the sample holder is fixed to a high precision spindle. The rotation of this splindle is controlled with a brushless synchronous motor allowing rotational speeds from 0.001 to 1000 rpm. Speed and position of the spindle are measured at high frequency with a high resolution encoder from Renishaw allowing a resolution as low as 0.001°. On the top plate, different modules can be installed. For this study, the sample was attached to the free extremity of a dual cantilever strain gage force sensor (SUP1-100N), allowing direct measurements of the forces applied to the sample without any losses in mechanical joints. The sensors are connected to dedicated electronic amplifiers (DAQ-P module Bridge-A from Dewetron). The noise obtained with this system was as low as 0.05N@1kHz on both normal and tangential forces. This system is positioned in height with a ball bearing screw controlled with a brushless synchronous motor. Forces can, therefore, be controlled through a computer in closed loop. This automatic control of the applied normal force allows good and fast runs. The sample vibration can be measured by a vibrometer Polytech OFV 505 (wavelength of 633 nm, frequency range 0.5 Hz–250 kHz) targeted to the fixed elastomer sample. This apparatus gives access to both displacement and velocity of the sample.

Forces, displacement and velocities are recorded with a computer using a 16 bit National Instrument acquisition board (NI PCI-6221). Data can then be extracted from the recorded file. Friction coefficient is directly obtained by dividing the tangential force by the normal force.

3.2 Protocol

All experiments have been performed in air and at ambient temperature. The sample length is 3 cm. Samples are not cleaned in order to avoid any damage of the surface treatment. Before each test, the disc is placed successively in ultrasonic baths of heptane, isopropanol and acetone. The wiper blade is put into contact against the silica disc with a controlled static force of 0.5 N (which results in a 16 N/m distribution of force per unit of length in the blade direction). The part of the blade in contact is the 90° edge of the lip, where the surface treatment is usually applied (Fig. 6). The tests are realised in wet condition. The lubricant consists of distilled water which is regularly injected into the contact during the test. The sliding velocity V of the disc at the contact point increases incrementally from 10 mm/s to 1 m/s. At each step, several measurements are realised successively and averaged during 5 s. The two force signals are recorded giving access to the friction coefficient versus sliding velocity (friction

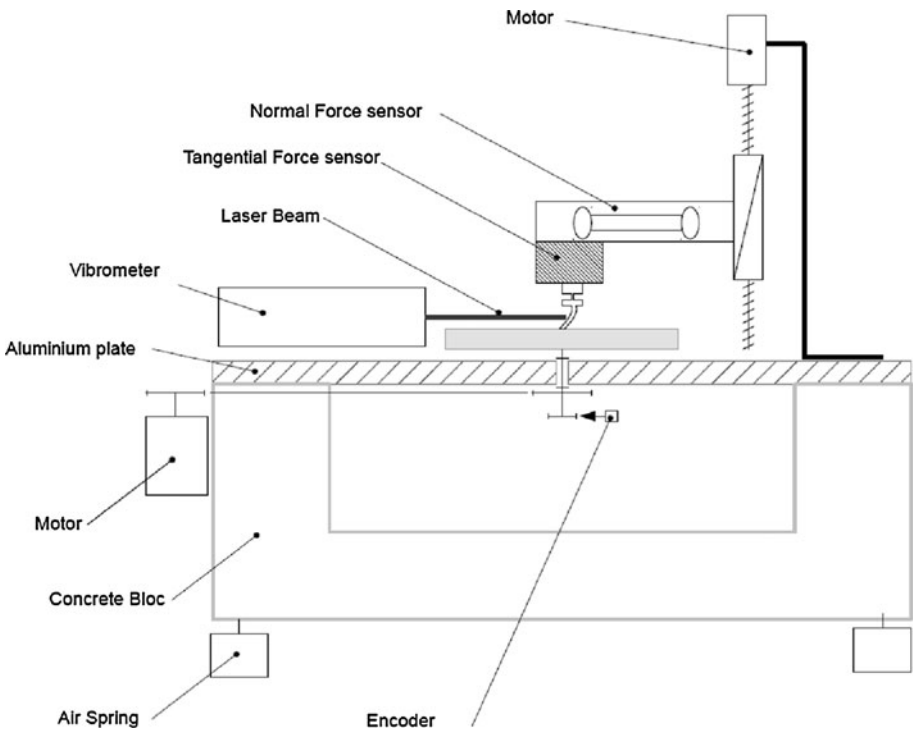

Fig. 5 Schematic diagram of tribometer LUG

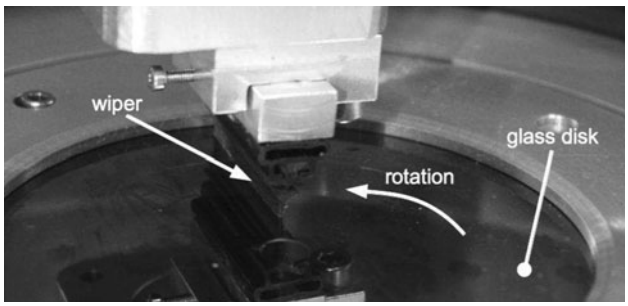

Fig. 6 Wiper blade/glass disc contact

coefficient is the 5 s average of tangential force divided by the normal force). The Stribeck curve is then obtained. In the same time, the laser vibrometer signal delivers the magnitude of the friction-induced displacement (if any) versus sliding velocity. The maximum amplitude of vibration is considered for each velocity. All friction measurements have been realised 5 times for each sample. The presented values are averages.

4 Results

Three samples referenced by the letters A, B and C have been tested. The measured friction coefficients versus sliding speed are shown in Figs. 7a, 8a and 9a. The error bars correspond to the highest and the lowest values obtained in 5 measurements. The values of the master curve parameters for the best fits of Stribeck's curve obtained with Matlab and Ezyfit toolbox are given in Table 1. For each sample, the three regimes boundary, mixed and hydrodynamic are clearly apparent. For low sliding velocities from 10 mm/s up to over 100 mm/s, the friction coefficient is almost constant about 0.5 ($G\eta^l$ in Table 1). The exponents l given in Table 1 have small values compared with unit which leads to a very weak dependance with the sliding speed in the boundary regime. The transition speed is 120 mm/s for samples A and B but 225 mm/s for sample C (U/η in Table 1). The transition of sample C is, therefore, shifted towards higher sliding velocities. Despite the fact that samples A and B have the same transition speed, the velocity range during which the transition occurs is wider for sample B than it is for sample A. This can be compared with the values of exponent r. The lower r the wider the transition. For sample B r is approximately 1, whilst it is 1.7 for sample A. Sample C has the narrowest transition with $r \sim 2.7$. The third regime (EHL) is not well explored. The complete observation of this regime and in particular the velocity strengthening would require measurements at large sliding velocities which are beyond the range of application of the experimental setup.

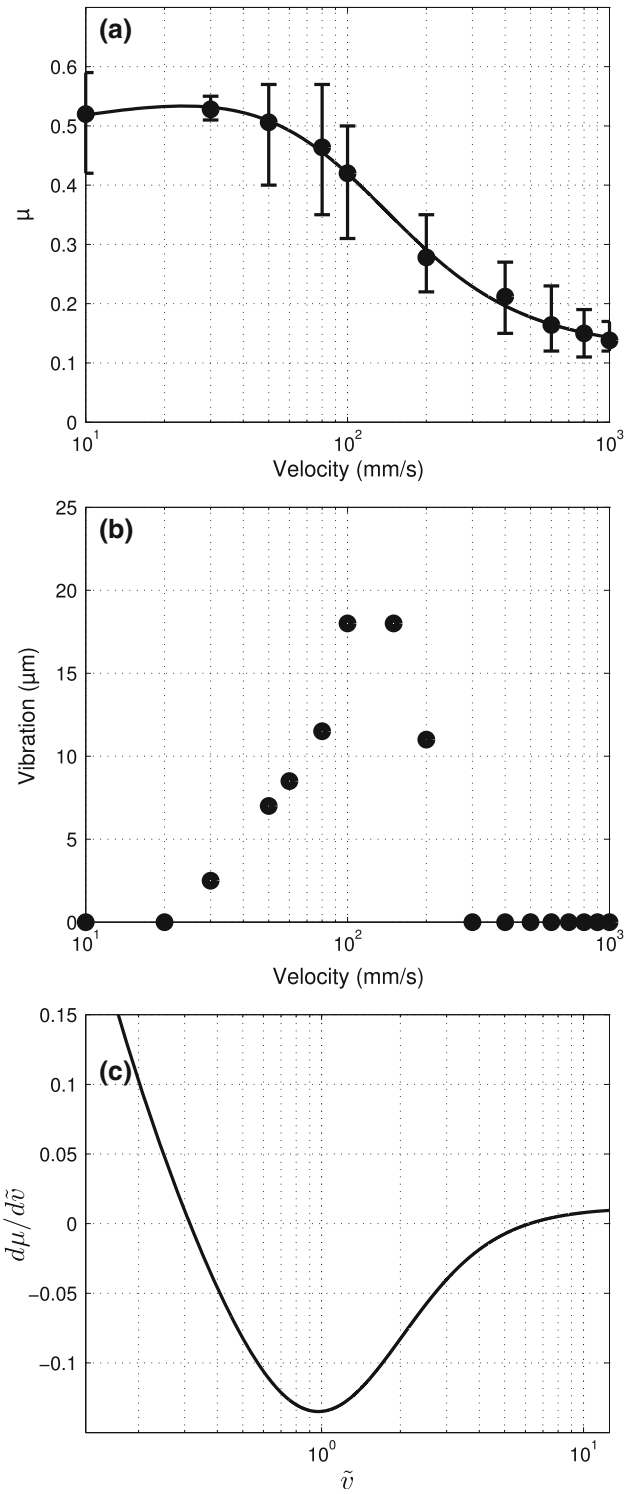

Fig. 7 Sample A: *filled circle* measurements; *dash* best fit. **a** Friction coefficient versus sliding velocity. **b** Vibration amplitude versus dimensionless velocity. **c** Slope of the empirical fit translated by 2ζ with $\zeta = 0.006$

The amplitude of vibration measured by the laser vibrometer varies from several micrometres to some tens of micrometres for the three tested samples. The frequency is

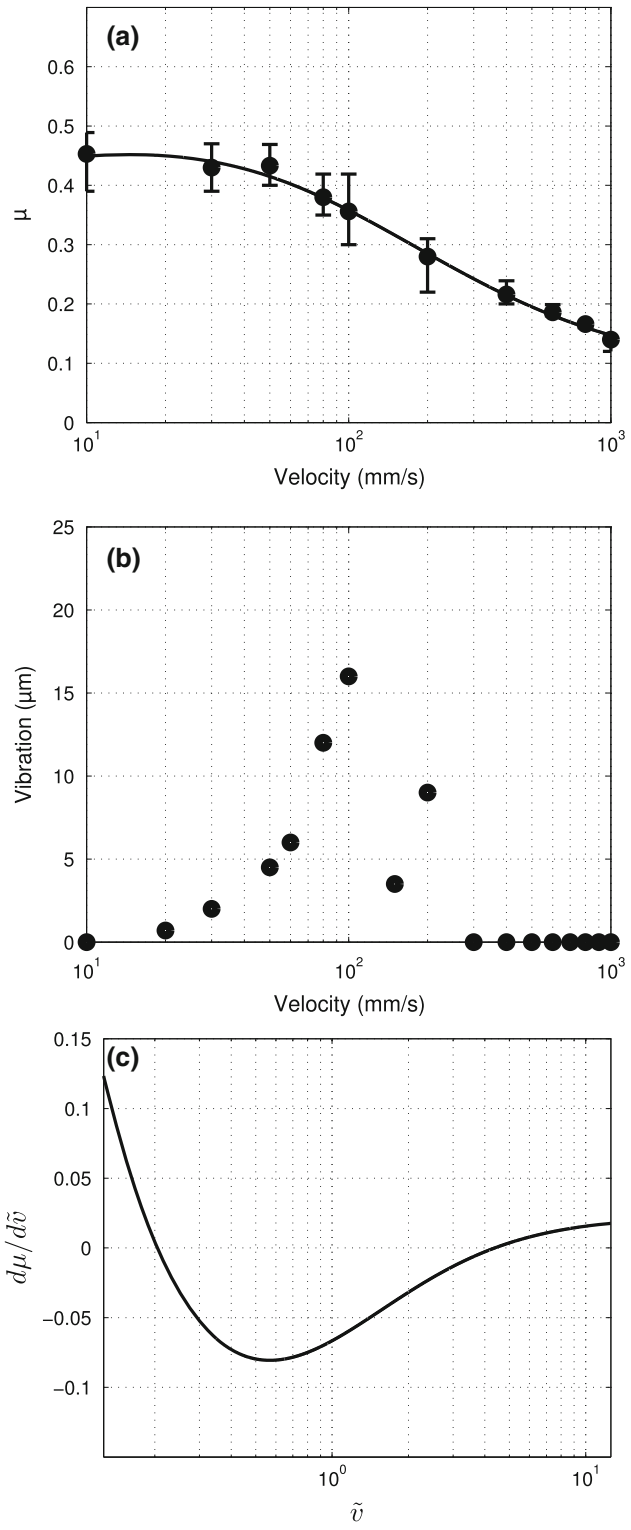

Fig. 8 Sample B: *filled circle* measurements; *dash* best fit. **a** Friction coefficient versus sliding velocity. **b** Vibration amplitude versus dimensionless velocity. **c** Slope of the empirical fit translated by 2ζ with $\zeta = 0.011$

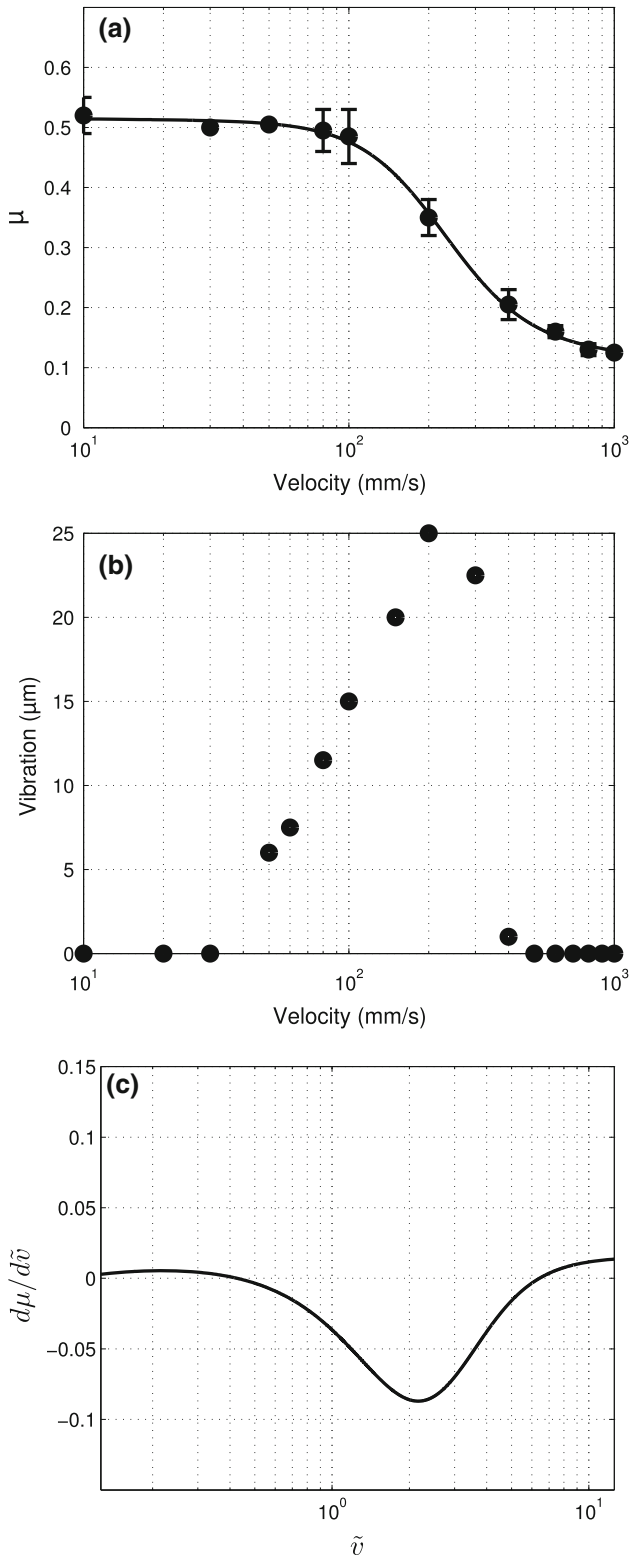

Fig. 9 Sample C: *filled circle* measurements; *dash* best fit. **a** Friction coefficient versus sliding velocity. **b** Vibration amplitude versus dimensionless velocity. **c** Slope of the empirical fit translated by 2ζ with $\zeta = 0.008$

about 700–900 Hz. For all samples, no vibration occurs at low velocity and of course no noise is emitted. The system is stable. At high velocities, the system is also stable and no noise emission is recorded. But for all samples, a strong vibration is observed for intermediate values of the sliding velocity. Most of the time, the vibration is not constant with time. The blade can vibrate for a short period, then stop and vibrate again, depending on sample and velocity. An example of the recorded displacement of sample A is given in Fig. 10. The periodic apparition and extinction of the limit cycle are related to the frequency of rotation of the disc and can be explained by a change in normal load due to a misalignment. One notices that the observed friction-induced vibration never has a stick phase, as shown in Fig. 11. The signal is almost perfectly sinusoidal. A similar behaviour has been observed for all samples. The amplitudes of the limit cycle in our case might be too small to reach a stick-slip regime [30]. The power spectral density of the signal is shown in Fig. 12, where a strong peak between 800 and 900 Hz is found.

The maximal vibration measurements as a function of velocity for the three samples are displayed in Figs. 7b, 8b and 9b.

In Figs. 7c, 8c and 9c, the derivative $d\mu/d\tilde{v}$ of the Stribeck's fit vertically shifted by the value 2ζ are shown. The correspondence between physical velocities and dimensionless velocities has been computed with the following parameters: mass $m = 1$ g, $\omega = 6383$ rad/s, $k = m\omega^2$ and $N = 0.5$ N. The x-axis of figures (a), (b) and (c) are aligned such that physical speeds of figures (a) and (b) are in correspondence with dimensionless speeds of figure (c). A negative value of the curve in Figs. 7c, 8c and 9c means that $d\mu/d\tilde{v} < -2\zeta$ and, therefore, the system is expected to be unstable.

For each sample, apparition and vanishing points of squeal noise occur for almost the same level of slope $d\mu/d\tilde{v}$. This can be observed by comparing the relevant sliding velocities in Figs. 7b, 8b and 9b with the corresponding values of $d\mu/d\tilde{v}$ in Figs. 7c, 8c and 9c. Furthermore, this common value of $d\mu/d\tilde{v}$ provides an assessment of the parameter ζ. In Table 2 the range of velocities of the squeal noise, the identified value of ζ and the strength of the vibration are summarized. The fact that the squeal noise appears and disappears at the same gradient of friction confirms the relevance of the stability criterion given in Eq. (12).

Table 1 Values of parameters for the fit of Stribeck's curves

Sample	$G\eta^l$	$H\eta^n$	U/η	l	n	r
A	0.443	0.169	122.47	0.071	−0.041	1.706
B	0.385	0.023	119.64	0.104	0.137	0.948
C	0.517	0.249	225.68	−0.0028	−0.104	2.723

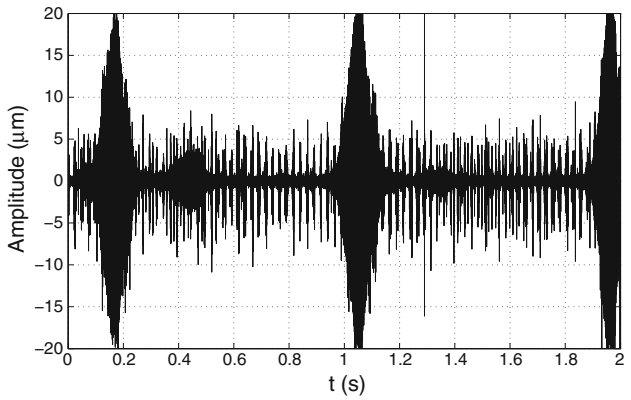

Fig. 10 Displacement signal of sample A blade as a function of time

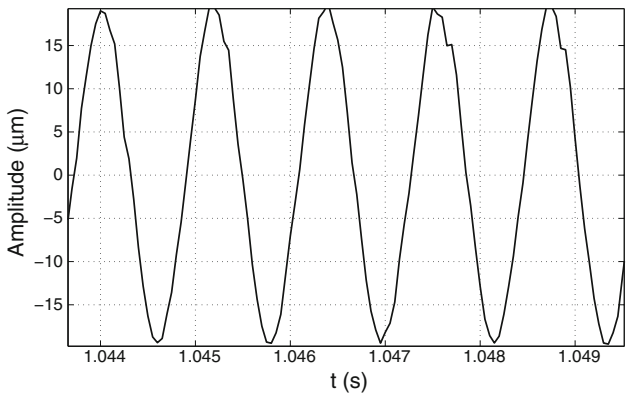

Fig. 11 Vibration of sample A blade

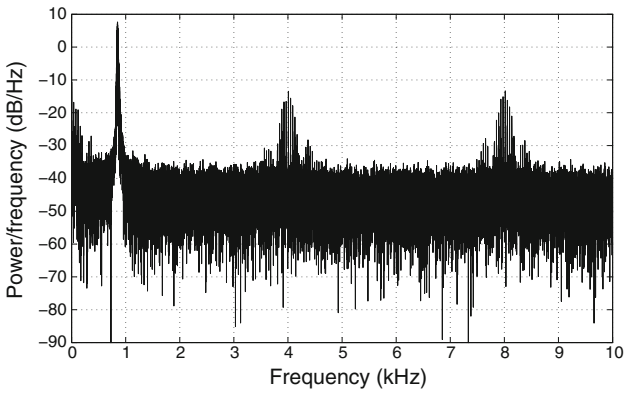

Fig. 12 Power spectral density of the vibration signal of sample A

Table 2 Range and intensity of squeal noise

Sample	Range (mm/s)	Dimensionless range	ζ	Vibration (µm)
A	20–300	0.25–4	0.006	18
B	10–300	0.1–4	0.011	16
C	30–500	0.4–6	0.008	25

For all samples, the vibration amplitude increases with velocity, reaches a maximum and then decreases. It seems significant that the maximum vibration corresponds to the inflection point of the Stribeck curve, characterised by the parameter U. Indeed, Stribeck's law should not be relevant as soon self-excited vibrations appear (except when averaged over time) [31].

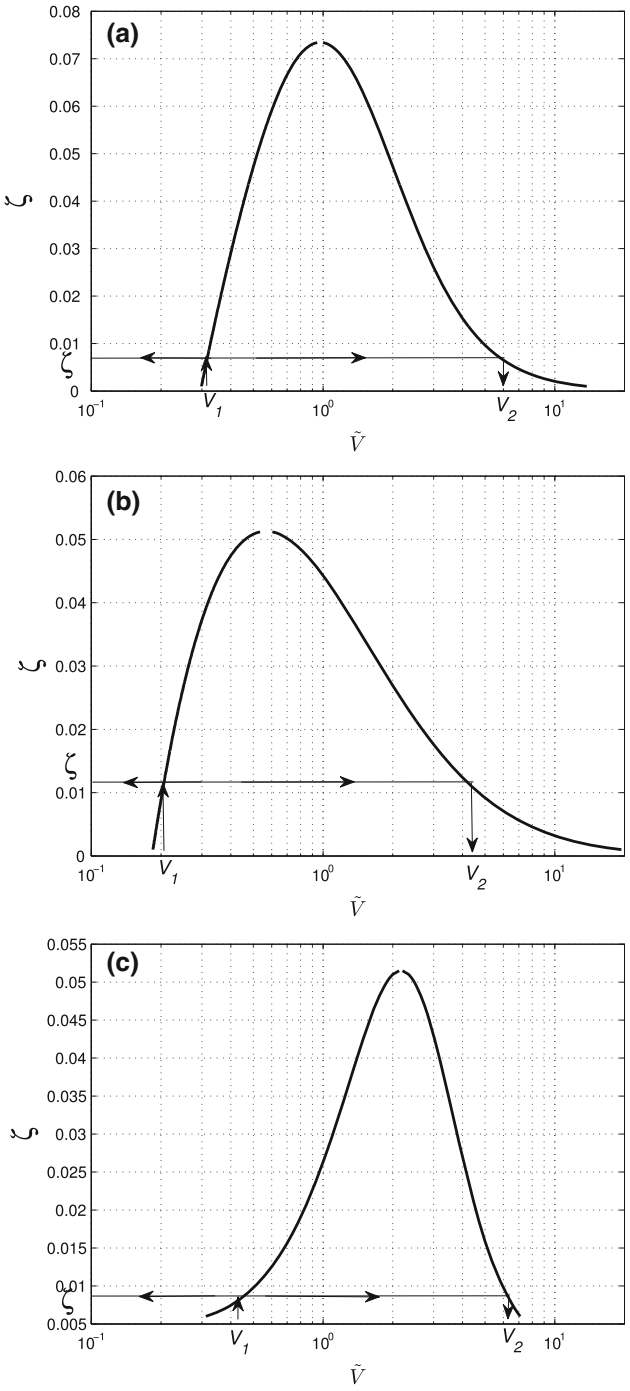

Fig. 13 Instability range: The lowest unstable velocity V_1 gives the damping factor ζ as well as the highest unstable velocity V_2. **a** Sample A. **b** Sample B. **c** Sample C

In Fig. 13a–c, the instability range of velocity is plotted as a function of the damping factor ζ. For a fixed ζ, the intersection of the curve with the line $y = \zeta$ line gives the boundary velocities of the unstable range. On the other hand, if the lowest unstable velocity V_1 is measured, the Stribeck curve and the stability criterion give access to both the damping factor ζ and the highest unstable velocity V_2.

5 Conclusion

In this paper, it has been shown that the squeal noise of wiper blades observed during the transition regime may be explained by a simple mathematical model. The most important result concerns the prediction of the velocity range of instabilities. Based on the stability analysis of a single degree of freedom submitted to a friction force which follows the Stribeck law, the criterion given in Eq. (12) has been derived. It shows that stationary measurements of friction coefficient versus sliding velocity can be employed to explain the apparition of squeal noise. A good accuracy has been achieved thanks to the selection of a suitable Stribeck curve fit taken from Bongaerts et al. Instability occurs when the negative gradient of the curve is steep enough. The threshold is fixed by the value ζ of the modal damping factor, a parameter which is usually unknown.

Several parameters control the shape of the Stribeck curve. Their values are imposed by the physical state of the contact. This suggests that it would be possible to control the apparition of squeal noise or to reduce its level by modifying the Stribeck curve. This could be achieved by tuning the interface between glass and rubber, for instance with an adapted surface treatment strategy, by choosing an appropriate surface coating or by optimizing the roughness of wiper lip [32]. Several strategies are possible such as shifting the transition speed to a higher value or reducing the maximum gradient of the curve.

Acknowledgments This work was funded by French government support through the RIBEG project (FUI 8 program).

References

1. Koenen, A., Sanon, A.: Tribological and vibroacoustic behavior of a contact between rubber and glass (application to wiper blade). Tribol. Int. **40**, 1484–1491 (2007)
2. Chevennement-Roux, C., Dreher, T., Alliot, P., Aubry, E., Laine, J.P., Jezequel, L.: Flexible wiper system dynamic instabilities: modelling and experimental validation. Exp. Mech. **47**, 201–210 (2007)
3. Fujii, Y.: Method for measuring transient friction coefficients for rubber wiper blades on glass surface. Tribol. Int. **41**, 17–23 (2008)

4. Bodai, G., Goda, T.J.: Friction force measurement at windscreen wiper/glass contact. Tribol. Lett. **45**, 515–523 (2012)
5. Akay, A.: Acoustics of friction. J. Acoust. Soc. Am. **111**, 1525–1548 (2002)
6. Butlin, T., Woodhouse, J.: A systematic experimental study of squeal initiation. J. Sound Vibrat. **330**, 5077–5095 (2011)
7. Vola, D., Raous, M., Martins, J.A.C.: Friction and instability of steady sliding: squeal of rubber/glass contact. Int. J. Numer. Methods Eng. **46**, 1699–1720 (1999)
8. Nayfeh, A.H., Mook, D.T.: Nonlinear oscillations. Wiley Interscience. 704 p. (1979).
9. Ibrahim, R.A.: Friction-induced vibration, chatter, squeal, and chaos. Appl. Mech. Rev. **47**, 209–253 (1994)
10. Denny, M.: Stick-slip motion: an important example of self-excited oscillation. Eur. J. Phys. **25**, 311–322 (2004)
11. Den Hartog, J.P.: Forced vibrations with combined coulomb and viscous friction. Trans. ASME **53**, 107–115 (1931)
12. Nakano, K.: Two dimensionless parameters controlling the occurence of stick-slip motion in a 1-DOF system with coulomb friction. Tribol. Lett. **24**, 91–98 (2006)
13. Scheibert, J., Dysthe, D.K.: Role of friction-induced torque in stick-slip motion. Europhys. Lett. **92**, 54001 (2010)
14. Ruina, A.L.: Instability and state variable friction laws. J. Geophys. Res. **88**, 359–370 (1983)
15. Baumberger, T., Berthoud, P., Caroli, C.: Physical analysis of the state-and rate-dependent friction law. II. Dynamic friction. Phys. Rev. B **60**, 3928–3939 (1999)
16. Dieterich, J.H.: Modeling of rock friction.1. Experimental results and constitutive equations. J. Geophys. Res. **84**, 2161–2168 (1979)
17. Rice, J.R., Ruina, A.L.: Stability of steady frictional slipping. J. Appl. Mech., Trans. of ASME. **50**, 343–349 (1983)
18. Baumberger, T., Caroli, C., Perrin, B., Ronsin, O.: Non-Linear analysis of the stick-slip bifurcation in the creep-controlled regime of dry friction. Phys. Rev. E **51**, 4005–4010 (1995)
19. Tromborg, J., Scheibert, J., Amundsen, D.S., Thogersen, K., Malthe-Sorenssen, A.: Transition from static to kinetic friction: insights from a 2D model. Phys. Rev. Lett. **107**, 074301 (2011)
20. Sugita, M., Yabuno, H., Yanagisawa, D.: Bifurcation phenomena of the reversal behavior of an automobile wiper blade. Nonlinear Dyn. **69**, 1111–1123 (2012)
21. Goto, S., Takahashi, H., Oya, T.: Clarification of the mechanism of wiper blade rubber squeal noise generation. JSAE Rev **22**, 57–62 (2001)
22. Deleau, F., Mazuyer, D., Koenen, A.: Sliding friction at elastomer/glass contact: influence of the wetting conditions and instability analysis. Tribol. Int. **42**, 149–159 (2009)
23. Tu, C.F., Fort, T.: A study of a fiber capstan friction. Part 1. Stribeck curves, part 2. Stick-slip phenomena. Tribol. Int. **37**, 701–719 (2004)
24. Heslot, F., Baumberger, T., Perrin, B., Caroli, B., Caroli, C.: Creep, stick-slip, and dry-friction dynamics: experiments and a heuristic model. Phys. Rev. E **49**, 4973–4990 (1994)
25. Dieterich, J.H.: Time-dependent friction and the mechanics of stick-slip. Pure Appl. Geophys. **116**, 790–806 (1978)
26. Gu, J.-C., Rice, J., Ruina, A.L., Tse, S.T.: Slip motion and stability of a single degree of freedom elastic system with rate and state dependent friction. J. Mech. Solids **32**, 167–196 (1984)
27. Smith, J.H., Woodhouse, J.: The tribology of rosin. J. Mech. Phys. Solids. **48**, 1633–1681 (2000)
28. Canudasde Vit, C., Olsson, H., Astrom, K.J., Lischinsky, P.: A new model for control of systems with friction. IEEE Trans. Automat. Contr. **40**, 419–425 (1995)
29. Bongaerts, J.H.H., Fourtouni, K., Stokes, J.R.: Soft-tribology: lubrication in a compliant PDMS–PDMS contact. Tribol. Int. **40**, 1531–1542 (2007)
30. Papenhuyzen, P.J.: Wrijvingsproeven in verband met het slippen van autobadden. De Ingenieur **V75 53**, 75–81 (1938)
31. Polycarpou, A.A., Soom, A.: Application of a two-dimensional model of continuous sliding friction to stick-slip. Wear **181–183**, 32–41 (1995)
32. Galda, L., Pawlus, P., Sep, J.: Dimples shape and distribution effect on characteristics of Stribeck curve. Tribol. Int. **42**, 1505–1512 (2009)